Institut für Reaktorwerkstoffe

KERNFORSCHUNGSANLAGE JÜLICH

des Landes Nordrhein-Westfalen

SURFACE EFFECTS ASSOCIATED WITH DISLOCATIONS IN LAYER CRYSTALS

von

R. Siems, P. Delavignette u. S. Amelinckx

Jül - 64 - RW

September 1962

Berichte der Kernforschungsanlage Jülich – Nr. 64

Institut für Reaktorwerkstoffe Jül – 64 – RW

Dok.: SURFACE EFFECTS
DISLOCATIONS
LAYER CRYSTALS
DK: 548.74.015.2

Zu beziehen durch: ZENTRALBIBLIOTHEK der Kernforschungsanlage Jülich,
Jülich, Bundesrepublik Deutschland

phys. stat. sol. 2, 636 (1962)

Studiencetrum voor Kernenergie, Mol

Surface Effects Associated with Dislocations in Layer Crystals

By

R. SIEMS[1]), P. DELAVIGNETTE and S. AMELINCKX

Dislocation configurations in thin foils cannot be accurately interpreted unless the effects of anisotropy and surfaces on the stresses and energies of edge and screw dislocations are known. Expressions for these effects are derived here for a semi-infinite hexagonal crystal with dislocations in the basal plane.

It is then shown that in plate-like crystals, as used in electron-microscopic investigations, the finite thickness of the specimen leads to observable effects on the dislocation patterns. In particular, the width of a ribbon decreases as it approaches the surface, due to the reduced repulsion between the partials, so that care is needed in deducing stacking fault energies from ribbon widths. Also the energy of a dislocation is a function of its distance from a surface, so that if it is crossed by a surface step it suffers a "refraction" which, in simple cases, follows Snell's law. It is further shown that dislocations will tend to be aligned with surface steps, and the interaction energy between a step and a parallel dislocation line can thus be derived from experimental data.

Finally, a method is suggested for obtaining information on the elastic constants from electron microscopic data.

Für eine richtige Interpretation von Versetzungs-Konfigurationen in dünnen Schichten sind Ausdrücke für die Spannungen und Energien von Stufen- und Schraubenversetzungen erforderlich, die die Anisotropie und das Vorhandensein von Oberflächen berücksichtigen. In der vorliegenden Arbeit werden solche Beziehungen für einen einseitig unendlichen hexagonalen Kristall mit Versetzungen in der Basisebene abgeleitet.

Es wird gezeigt, daß bei plattenförmigen Kristallen, wie sie für elektronenmikroskopische Untersuchungen verwendet werden, die endliche Dicke zu beobachtbaren Effekten in der Versetzungs-Anordnung führt. Insbesondere nimmt die Breite von Stapelfehler-Bändern in der Nähe der Oberfläche ab infolge der verminderten Abstoßung zwischen den Teilversetzungen. Demzufolge ist bei der Bestimmung von Stapelfehlerenergien aus der Breite der Bänder Vorsicht geboten. Da die Selbstenergie einer Versetzung eine Funktion ihres Abstandes von der Oberfläche ist, tritt eine „Brechung" auf, wenn die Versetzung eine Oberflächenstufe kreuzt. Im einfachsten Fall ist das Snellius'sche Gesetz gültig. Es wird gezeigt, daß Versetzungen das Bestreben haben, sich parallel zu Oberflächenstufen auszurichten. Die Wechselwirkungsenergie zwischen einer Stufe und einer parallelen Versetzung kann experimentell bestimmt werden.

Es wird eine Methode vorgeschlagen, mit deren Hilfe aus elektronenmikroskopischen Beobachtungen Aussagen über die elastischen Konstanten gewonnen werden können.

1. Introduction

The question whether the influence of the finite specimen thickness on the geometry of dislocation patterns observed in thin foils is important or not, has often been raised. The layer structures are a specially convenient medium to study quantitatively certain aspects of such influences in a particularly simple geometry.

[1]) Permanent address: Institut für Reaktorwerkstoffe, Kernforschungsanlage Jülich

The dislocations in most layer structures are all exactly parallel to the basal plane, which is usually the specimen plane, if the foil was prepared by cleavage or by growth from the vapour phase. Many layer structures show furthermore extended dislocations, since the stacking fault energies are usually small. Such stacking fault ribbons, if wide enough, are particularly useful "probes". The two partials are kept together by a constant force γ, which does not depend on the distance between partials, nor on the distance from a free surface. It is numerically equal to the stacking fault energy if corresponding units are chosen. On the other hand, the repulsion between the partials is proportional to the inverse of their distance in an infinite isotropic solid. For ribbons in the vicinity of the surface of a semi-infinite solid, the repulsion law has to be corrected for surface effects. It is desirable, therefore, to obtain analytical expressions for the stress fields of edge and screw dislocations parallel to a free surface, taking into account these surface effects as well as the anisotropy. This is important if one wants to use these ribbons for measurements of stacking fault energies.

Analytical expressions for the stress field were given for arbitrary dislocations in isotropic semi-infinite media and in plates by DIETZE and LEIBFRIED [1], in infinite anisotropic materials by ESHELBY et al [2] and by SEEGER and SCHOECK [3]. For the special case of dislocations in the basal plane of infinite hexagonal crystals, formulae were given by SPENCE [4] and BAKER et al [5], and for screw dislocations in plates of hexagonal materials by SPENCE [6] and by SIEMS [7]. In the present paper the stress field will be obtained for screw- and for edge-dislocations with Burgers vectors and dislocation lines in the basal plane of a semi-infinite hexagonal crystal. As in most practical applications interactions between dislocations in the same basal lattice plane are discussed, the stress field in this plane will be plotted for several values of the elastic constants. The stress field of a dislocation in a plate may be replaced by the expression for the stress field of a dislocation in a semi-infinite material if the distances to the nearest surface are taken to be equal. The conditions under which this method gives reliable results will be discussed after the formulae have been derived.

We will further obtain expressions for the self-energy of the dislocations.

Applications to observed effects in a few layer structures will also be mentioned briefly, while a more detailed comparison of the theory with the observations will be made in another paper.

2. The Width of Dislocation Ribbons in an Infinite Isotropic Solid

Putting the repulsion forces equal to the attraction exerted by the stacking fault, one obtains the following relation which determines the equilibrium separation

$$ {}^1b_E\,{}^2\tau_{x\,z,\,E}(0) + {}^1b_S\,{}^2\tau_{y\,z,\,S}(0) = +\gamma \qquad (1) $$

(b is the Burgers vector of the partial dislocation)

or an equivalent one by interchanging the upper indices 1 and 2. This expression is general and also valid in the anisotropic, finite case, provided the right expressions for τ_{xz} and τ_{yz} are used. The subscripts E and S refer to edges and screws respectively, whilst the left indices 1 and 2 refer to partials (1) and (2). The ex-

pressions for τ_{xz} and τ_{yz} have to be taken for $z = 0$, i. e. in the glideplane. In an infinite isotropic solid the expressions for $\tau_{xz,E}$ and $\tau_{yz,S}$ are

$$\tau_{xz,E} = \frac{\mu b}{2\pi(1-\nu)} \cdot \frac{x(x^2-z^2)}{(x^2+z^2)^2}; \tag{2}$$

$$\tau_{yz,S} = \frac{\mu b}{2\pi} \cdot \frac{x}{(x^2+z^2)}. \tag{3}$$

From these relations the well known formula for the distance between partials in an infinite isotropic medium is easily obtained

$$d = d_0\left(1 - \frac{2\nu}{2-\nu} \cdot \cos 2\Phi\right); \tag{4}$$

$$d_0 = \frac{\mu b^2}{8\pi\gamma} \cdot \frac{2-\nu}{1-\nu}, \tag{5}$$

where Φ is the angle between the total Burgers vector and the direction of the ribbon.

The total width of the symmetrical double ribbon in an isotropic infinite crystal is given by [8]

$$w = w_0\left(1 - \frac{\nu}{2-\nu} \cdot \cos 2\Phi\right), \tag{6}$$

$$w_0 = \frac{3\mu b^2}{4\pi\gamma} \cdot \frac{2-\nu}{1-\nu}. \tag{7}$$

3. Stress Field in an Infinite Anisotropic Crystal

We shall use a system of cartesian coordinates with the z-axis parallel to the hexagonal axis; the dislocation is parallel to the y-axis at $z = \zeta$, $x = 0$. Using the notation of SPENCE [6] we can write the z-plane stress components in the form

$$\tau_{zy,S} = C_2 \cdot \frac{b_S x}{x^2 + \delta_3 (z-\zeta)^2}, \tag{8}$$

for screw dislocations and

$$\left.\begin{aligned} \tau_{zz,E} &= C_1 \frac{b_E (z-\zeta)\,[x^2 - \delta_1 (z-\zeta)^2]}{x^4 + \delta_2 x^2 (z-\zeta)^2 + \delta_1^2 (z-\zeta)^4}, \\ \tau_{zx,E} &= C_1 \frac{b_E x\,[x^2 - \delta_1 (z-\zeta)^2]}{x^4 + \delta_2 x^2 (z-\zeta)^2 + \delta_1^2 (z-\zeta)^4}, \end{aligned}\right\} \tag{9}$$

for edge dislocations. The Burgers vector lies in the basal plane.

In these equations the following abbreviations are used:

$$\left.\begin{aligned} &\delta_1 = \sqrt{\frac{c_{11}}{c_{33}}}; \qquad \delta_2 = \frac{c_{11}c_{33} - c_{13}^2 - 2c_{13}c_{44}}{c_{33}c_{44}}; \qquad \delta_3 = \frac{c_{66}}{c_{44}}; \\ &C_1 = \frac{c_{11}c_{33} - c_{13}^2}{2\pi c_{33}(2\delta_1 + \delta_2)^{1/2}}; \qquad C_2 = \frac{1}{2\pi}\sqrt{c_{44}c_{66}}; \qquad c_{66} = \frac{1}{2}(c_{11} - c_{12}). \end{aligned}\right\} \tag{10}$$

We shall further use $\Delta = \delta_2/\delta_1$;
b_E and b_S are the edge- and screw-components of the Burgers vector.

From these expressions for $\tau_{zy,S}$ and $\tau_{zx,E}$ and formula (1) the width of a ribbon in the c-plane of an infinite anisotropic crystal with hexagonal symmetry can easily be found

$$d = d_0\left(1 + 2\frac{C_2 - C_1}{C_2 + C_1}\cos 2\Phi\right), \tag{11}$$

with

$$d_0 = \frac{b^2 (C_1 + C_2)}{4\gamma}. \tag{12}$$

This formula is equivalent to that given by BAKER et al [5].

For the equilibrium width w of a symmetrical double ribbon, one finds

$$w = w_0\left(1 + \frac{C_2 - C_1}{C_2 + C_1}\cos 2\Phi\right), \tag{13}$$

with

$$w_0 = \frac{3\, b^2 (C_1 + C_2)}{2\gamma}. \tag{14}$$

4. Stress Field for a Screw Dislocation in a Semi-Infinite Medium

The stress field for a screw dislocation (see Fig. 1) can be obtained quite easily by superposing the stress field of a mirror dislocation of opposite sign

$$\tau_{zy,S} = C_2 b_S\left[\frac{x}{x^2 + \delta_3 (z - \zeta)^2} - \frac{x}{x^2 + \delta_3 (z + \zeta)^2}\right].$$

The $\tau_{zy,S}$ components cancel at $z = 0$, making the surface stress-free. Introducing a new scale factor for the z-direction according to

$$z' = \sqrt{\delta_3}\, z\,; \qquad \zeta' = \sqrt{\delta_3}\,\zeta\,; \tag{15}$$

one obtains

$$\tau_{zy,S} = C_2 b_S\left[\frac{x}{x^2 + (z' - \zeta')^2} - \frac{x}{x^2 + (z' + \zeta')^2}\right]. \tag{16}$$

At points in the plane $z = \zeta$, i. e. $z' = \zeta'$, this reduces to

$$\tau_{zy,S} = \frac{C_2 b_S}{x}\left[1 - \frac{1}{1 + 4v'}\right] \equiv \frac{C_2 b_S}{x}[1 - f] \tag{17}$$

with

$$\frac{z'}{x} = \sqrt{v'} \qquad \text{and} \qquad \frac{z}{x} = \sqrt{v} = \sqrt{\frac{v'}{\delta_3}}. \tag{18}$$

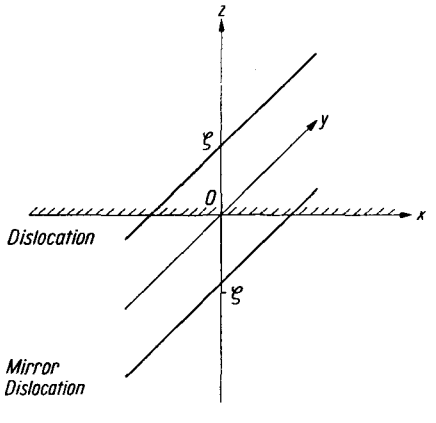

Fig. 1. A dislocation and a mirror dislocation on either side of the surface of a semi-infinite solid

5. Stress Field for an Edge Dislocation in a Semi-Infinite Medium

By superposing the stress field of a mirror dislocation of opposite sign (Fig. 1), we may again obtain a surface free of shear stress. The normal stresses, however, have the same sign at the surface and, therefore, the τ_{zz} component does not vanish.

The surface stresses due to the dislocation and the mirror dislocation are

$$\tau_{zx}^{M} = 0\,; \qquad \tau_{zz}^{M} = -\,2\,C_1\,b_E\,\frac{\zeta\,(x^2 - \delta_1\,\zeta^2)}{x^4 + \delta_2\,x^2\,\zeta^2 + \delta_1^2\,\zeta^4}\,.$$

Changing the scale of the z-coordinate according to

$$\bar{z} = \sqrt{\delta_1}\,z; \qquad \bar{\zeta} = \sqrt{\delta_1}\,\zeta\,, \tag{19}$$

and introducing $\Delta = \delta_2/\delta_1$, we obtain

$$\tau_{zx}^{M} = 0\,; \qquad \tau_{zz}^{M} = -\,2\,C_1\,b_E\,\frac{\zeta\,(x^2 - \bar{\zeta}^2)}{x^4 + \Delta\,x^2\,\bar{\zeta}^2 + \bar{\zeta}^4}\,. \tag{20}$$

A compensating stress field has to be superposed having no singularities for $z > 0$, and whose stresses at $z = 0$ are opposite in sign to those given by (20), i. e.

$$\tau_{zx}^{C} = 0\,; \qquad \tau_{zz}^{C}(z=0) = 2\,C_1\,b_E\,\frac{\zeta\,(x^2 - \bar{\zeta}^2)}{x^4 + \Delta\,x^2\,\bar{\zeta}^2 + \bar{\zeta}^4}\,. \tag{20a, b}$$

Because of the independence of the problem with respect to the y-coordinate, the stress field can be derived from a function $F(x, z)$:

$$\tau_{xx}^{C} = F_{zz} = \frac{\partial^2 F}{\partial z^2}\,; \qquad \tau_{xz}^{C} = -\,F_{xz}\,; \qquad \tau_{zz}^{C} = F_{xx}\,.$$

In this way the equations of equilibrium are fulfilled. The function F has to be chosen so that the compatibility conditions be satisfied as well. With a trial solution

$$F = e^{i\,\alpha\,x + i\,\alpha\,\varkappa z} \tag{21}$$

these conditions give the allowed values of $\varkappa$ as solutions of the equation

$$S_{11}\,\varkappa^4 + (2\,S_{13} + S_{55})\,\varkappa^2 + S_{33} = 0\,, \tag{22}$$

with

$$S_{ki} = s_{ki}\,s_{11} - s_{k2}\,s_{i2}$$

Here the s_{ik} are the elastic moduli defined according to

$$\begin{pmatrix} \dfrac{\partial u}{\partial x} \\ \dfrac{\partial v}{\partial y} \\ \dfrac{\partial w}{\partial z} \\ \dfrac{\partial v}{\partial z} + \dfrac{\partial w}{\partial y} \\ \dfrac{\partial w}{\partial x} + \dfrac{\partial u}{\partial z} \\ \dfrac{\partial u}{\partial y} + \dfrac{\partial v}{\partial x} \end{pmatrix} = (s_{ik}) \begin{pmatrix} \tau_{xx} \\ \tau_{yy} \\ \tau_{zz} \\ \tau_{yz} \\ \tau_{zx} \\ \tau_{xy} \end{pmatrix}.$$

The s_{ik} are not the tensor components.

The solutions of equation (22) are

$$\varkappa_{1,2}^2 = -A \pm \sqrt{A^2 - B} = \sqrt{B}\left\{-\frac{A}{\sqrt{B}} \pm \sqrt{\frac{A^2}{B} - 1}\right\},$$

with

$$A = \frac{2\,S_{13} + S_{55}}{2\,S_{11}} \qquad \text{and} \qquad B = \frac{S_{33}}{S_{11}}.$$

Now

$$\frac{1}{2}\Delta = \frac{\delta_2}{2\,\delta_1} = \frac{c_{11}\,c_{33} - c_{13}^2 - 2\,c_{13}\,c_{44}}{2\,c_{44}\sqrt{c_{33}\,c_{11}}}.$$

Using the relation between the c_{ik} and the s_{ik}, it can be proved that

$$\frac{A}{\sqrt{B}} = \frac{\Delta}{2} \qquad \text{and} \qquad \sqrt{B} = \delta_1 = \sqrt{\frac{c_{11}}{c_{33}}}.$$

With the abbreviation

$$R_{1,2}^2 = \frac{\Delta}{2} \pm \sqrt{\frac{\Delta^2}{4} - 1}, \tag{23}$$

one obtains

$$\varkappa_1 = \pm\sqrt{\delta_1}\,R_1, \qquad \varkappa_2 = \pm\sqrt{\delta_1}\,R_2. \tag{24}$$

For $\Delta > 2$ ($\Delta = 78$ for graphite), R_1 and R_2 are real numbers which are chosen to be positive. The admissible values of the roots of equation (22) are determined by observing that the stress function has to give a finite stress for $z \to \infty$. Thus the general stress function can be represented by the following integral (see (21)).

$$F(x, z) = \int_{-\infty}^{\infty}\left\{A_1(\alpha)\,e^{-|\alpha|\,R_1\,\bar{z}} + A_2(\alpha)\,e^{-|\alpha|\,R_2\,\bar{z}}\right\} e^{i\,\alpha\,x}\,d\alpha. \tag{25}$$

The stresses are then given by

$$\tau_{zx}^C = -F_{zx} = i\sqrt{\delta_1}\int_{-\infty}^{\infty}\left\{\alpha\,|\alpha|\,R_1\,A_1\,e^{-|\alpha|R_1\bar{z}} + \alpha\,|\alpha|\,R_2\,A_2\,e^{-|\alpha|\,R_2\bar{z}}\right\} e^{i\,\alpha\,x}\,d\alpha, \tag{26}$$

and

$$\tau_{zz}^C = F_{xx} = -\int_{-\infty}^{\infty}\alpha^2\left\{A_1\,e^{-|\alpha|\,R_1\bar{z}} + A_2\,e^{-|\alpha|\,R_2\bar{z}}\right\} e^{i\,\alpha\,x}\,d\alpha. \tag{27}$$

In Appendix I the functions $A_1(\alpha)$ and $A_2(\alpha)$ are determined from the boundary conditions (20a, b).

Introducing these functions into equation (13), changing the limits of integration and collecting terms, one obtains

$$\tau_{zx}^C = \frac{C_1\,b_E}{(R_2 - R_1)^2}\,2\,\mathrm{Im}\int_0^{\infty}\{-e^{-\alpha\,(R_1\bar{\zeta} + R_1\bar{z} - i\,x)} + e^{-\alpha\,(R_1\bar{\zeta} + R_2\bar{z} - i\,x)} + e^{-\alpha\,(R_2\bar{\zeta} + R_1\bar{z} - i\,x)} - e^{-\alpha\,(R_2\bar{\zeta} + R_2\bar{z} - i\,x)}\}\,d\alpha.$$

Bearing in mind that $(R_2 - R_1)^2 = \Delta - 2$, one can express the z-plane components of the compensating stress field as follows:

$$\tau_{zx}^C = \frac{2\,C_1\,b_E}{\Delta - 2}\cdot\{I_{12} + I_{21} - (I_{11} + I_{22})\}, \tag{28}$$

and

$$\tau_{zz}^C = \frac{2\,C_1\,b_E}{\Delta - 2}\cdot\frac{1}{\sqrt{\delta_1}}\{(\bar{z} + R_1^2\,\bar{\zeta})\,I_{12} + (\bar{z} + R_2^2\,\bar{\zeta})\,I_{21} - (\bar{z} + \bar{\zeta})\cdot(I_{11} + I_{22})\}, \tag{29}$$

with

$$I_{ij} = \frac{1}{(R_i\,\bar{\zeta} + R_j\,\bar{z})^2 + x^2}\,.$$

The total stresses are obtained by adding the contributions from dislocation, mirror dislocation and the compensating stresses

$$\tau_{zx} = C_1\,b_E\,x\left\{N_- - N_+ + \frac{2}{\Delta - 2}\,[I_{12} + I_{21} - (I_{11} + I_{22})]\right\}, \tag{30}$$

$$\tau_{zz} = \frac{C_1\,b_E}{\sqrt{\delta_1}}\left\{(\bar{z} - \bar{\zeta})\,N_- - (\bar{z} + \bar{\zeta})\,N_+ + \frac{2}{\Delta - 2}\,[(\bar{z} + \bar{\zeta}\,R_2^2)\,I_{21} + (\bar{z} + \bar{\zeta}\,R_1^2)\,I_{12} - (\bar{z} + \bar{\zeta})\,(I_{11} + I_{22})]\right\}, \tag{31}$$

with

$$N_\pm = \frac{x^2 - (\bar{z} \pm \bar{\zeta})^2}{(\bar{z} \pm \bar{\zeta})^4 + \Delta\,(\bar{z} \pm \bar{\zeta})^2 + x^4}\,.$$

6. Discussion of the Stress Formulae

In Appendix II it is shown that the expressions (16) and (30) go over into the corresponding isotropy formulae of DIETZE and LEIBFRIED [1] if the elastic constants approach the isotropy values.

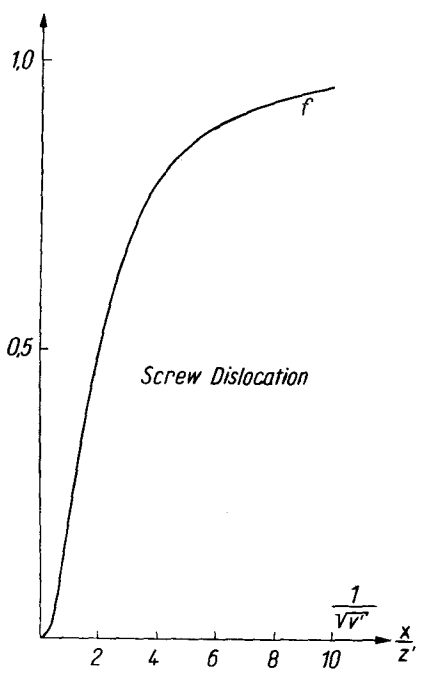

Fig. 2. The relative contribution of the mirror dislocation to the stress in the glide plane of a screw dislocation as a function of x/z' (x: distance from the dislocation, z': reduced distance from the surface)

In practical problems, the stress field is often needed for $z = \zeta$, i. e. for observation points in the glide plane of the dislocation. In this case, equation (17) reduces to

$$\tau_{zx} = \frac{C_1\,b_E}{x}\left\{1 - \frac{1 - 4\,\bar{v}}{1 + 4\,\Delta\,\bar{v} + 16\,\bar{v}^2} + \frac{2}{\Delta - 2}\left[\frac{2}{\bar{v}\,(\Delta + 2) + 1} - \frac{1}{4\,\bar{v}\,R_1^2 + 1} - \frac{1}{4\,\bar{v}\,R_2^2 + 1}\right]\right\}, \tag{32}$$

$$\tau_{zx} = \frac{C_1\,b_E}{x}\,[1 - g_s(\bar{v}) - g_k(\bar{v})] \tag{33}$$

with $\bar{v} = \bar{z}^2/x^2$.

It is seen from equations (17) and (33) that the factors by which the infinite material stress field has to be multiplied to give the stress for the semi-infinite medium are $1 - f$ or $1 - g_s - g_k$, respectively. In Fig. 2 and 3 the terms f from equation (17) for screw dislocations and g_s and g_k from equation (33) for edge dislocations are plotted as functions of $1/\sqrt{v'} = x/z'$ or $1/\sqrt{\bar{v}} = x/\bar{z}$, respectively,

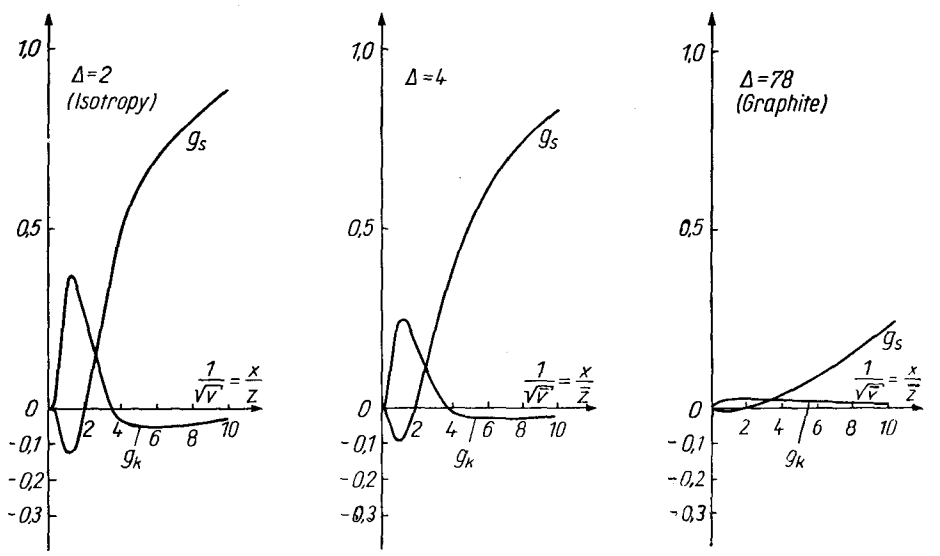

Fig. 3. The relative contributions of the mirror dislocation (g_s) and of the compensating field (g_k) to the stress in the glide plane of an edge dislocation as a function of $x/\bar{z}$ (x: distance from the dislocation, $\bar{z}$: reduced distance from the surface)

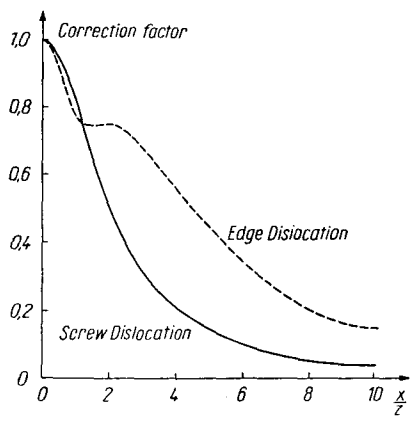

Fig. 4. Correction factors $(1-f)$ and $(1-g_k-g_s)$ for the stresses in the glide planes of an edge- and of a screwdislocation in isotropic material versus x/z (x: distance from the dislocation, z: distance from the surface)

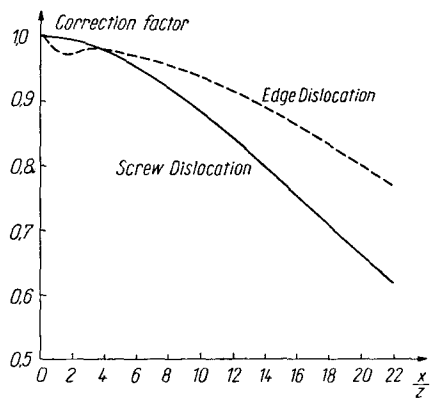

Fig. 5. Correction factors $(1-f)$ and $(1-g_k-g_s)$ for the stresses in the glide planes of an edge- and of a screwdislocation in graphite versus x/z (x: distance from the dislocation, z: distance from the surface)

for various values of Δ. We notice that the influence of the compensation stresses becomes the less important the larger the anisotropy, i. e. the larger the constant Δ. For graphite ($\Delta = 78$), for example, g_k is always less than 3%. For less anisotropic materials, however, the contribution of the compensation stresses may become larger than 30%. The position of the maximum of g_k depends only very little on Δ. It is located at values of $x/\bar{z}$ between 1 and 2.

In Fig. 4 and 5 the correction factors $1-f$ and $1-g_s-g_k$ are plotted for isotropic materials and for graphite as functions of x/z. For materials of moderate anisotropy, the correction factor for edge dislocations may be considerably smaller than the factor for screw dislocations. As a consequence, at a certain distance from

the surface, the repulsion between two screw dislocations may be stronger than that between edge dislocations, especially for materials for which the effective Poisson's ratio, given by $C_2/C_1 = 1 - \nu$ [8] is close to zero. In this case, screw ribbons will be wider than edge ribbons.

7. The Elastic Energy of Dislocations

The elastic stress field of a dislocation can be produced by removing the material from a cylinder of radius $R_i \approx b$ around the straight line $z = \zeta$, $x = 0$, cutting the medium along the plane $z = \zeta$ from $x = R_i$ to infinity, and displacing the two sides of the cut over a distance $\bar{b}$ relative to each other. The work necessary to perform this operation is obtained by integrating $\frac{1}{2}\, b\, \tau$ along the cut[2]).

For screw dislocations one obtains from equation (16)

$$E = C_2 \frac{b_S^2}{4} \left[\int_{R_i^2}^{\infty} \frac{dx^2}{x^2} - \int_{R_i^2}^{\infty} \frac{dx^2}{x^2 + 4\, z'^2} \right] = \frac{C_2\, b_S^2}{4} \ln \left\{ 1 + 4 \frac{z'^2}{R_i^2} \right\}.$$

As $z' \gg R_i$ in practical cases, one can neglect the first term in the logarithm

$$E = \frac{C_2\, b_S^2}{2} \ln 2 \frac{z'}{R_i} = \frac{C_2\, b_S^2}{2} \left[\ln \frac{2\, z}{R_i} + \frac{1}{2} \ln \delta_3 \right].^{3}) \tag{34}$$

For edge dislocations, on the other hand, one obtains from equation (30), by introducing $u = x^2/\bar{z}^2$, i. e. $x\, dx = \frac{1}{2}\, \bar{z}^2\, du$;

$$E = \frac{C_1\, b_E^2}{4} \left[\int_{\frac{R_1^2}{\bar{z}^2}}^{\infty} \left\{ \frac{1}{u} - \frac{u - 4}{u^2 + 4\, \Delta\, u + 16} + \frac{2}{\Delta - 2} \left(\frac{2}{\Delta + 2 + u} - \frac{1}{4\, R_1^2 + u} - \frac{1}{4\, R_2^2 + u} \right) \right\} du \right].$$

Performing the integration and assuming $\bar{z} \gg R_i$, yields

$$E = \frac{C_1\, b_E^2}{4} \left[2 \ln \frac{2\, \bar{z}}{R_i} + \frac{1}{2} \sqrt{\frac{\Delta + 2}{\Delta - 2}} \ln \frac{2\, \Delta + 2 \sqrt{\Delta^2 - 4}}{2\, \Delta - 2 \sqrt{\Delta^2 - 4}} - \frac{4}{\Delta - 2} \ln \frac{\Delta + 2}{4} \right]. \tag{35}$$

As in the case of the screw dislocation, the difference in energy of two dislocations at distances z_1 and z_2 from the surface depends on the elastic constants only through C_1

$$E_1 - E_2 = \frac{C_1\, b_E^2}{2} \ln \frac{z_1}{z_2}. \tag{36}$$

For isotropy ($\Delta \to 2$), expression (35) becomes

$$E = \frac{\mu\, b_E^2}{4\, \pi\, (1 - \nu)} \left[\ln \frac{2\, z}{R_i} + \frac{1}{2} \right].$$

---

[2]) The work performed at the inner surface is hereby neglected.

[3]) To obtain a consistent model, we may ask for a stress-free inner surface. It is convenient to cut out an elliptic cylinder around the dislocation. If the z-axis of the generating ellipse is made equal to $R_i/\sqrt{\delta_3}$ and the x-axis equal to R_i (with arbitrary R_i) this inner surface is stress-free. The energy is, in this case, given by equation (34).

For very anisotropic materials ($\Delta \gg 2$), on the other hand, the following expression is obtained

$$E = \frac{C_1 b_E^2}{4}\left[2\ln\frac{2z}{R_i} + \left(1 - \frac{2}{\Delta}\right)\ln\Delta + \ln\delta_1\right]. \quad (37)$$

The last two terms, which contain only anisotropy contributions, may represent a considerable fraction of the total energy. For a dislocation at a distance $z = 200\,R_i \cong 200\,b$ under the surface, in a material with $\Delta = 78$ and $\delta_1 = 5$ (graphite), the first term in the brackets is equal 12, the second 4.35, and the third 1.6, i. e. the two "anisotropy terms" contribute about $^1/_3$ of the total elastic energy.

A rigorous treatment of the dislocation core would yield stresses at the surface of the small cylinder around the dislocation, which are probably different from those given by equations (16), (30) and (31). The work due to the stresses at this surface is not contained in equations (34) and (35). Taking the boundary stresses at this surface into account would change the last term in equation (34) and the second and third terms in equation (35).

8. Application of the Semi-Infinite Space Formulae to Dislocations in a Plate

The equations derived above are expected to give a good approximation for the stress field in a plate under the following condition: if one takes for the surface of the semi-infinite space that side of the plate which is farther away from the dislocation, at the point in question the corrective terms (f in equation (17) and $g_s + g_k$ in equation (33)) must be small as compared to the leading term.

The quantity ζ to be introduced into the expressions for the stress field is then the distance to the nearest side of the plate. If a plate is so thick that a dislocation ribbon of a certain kind in its central plane has the width characteristic for the infinite medium, then the forces between the partials of any ribbon of this kind in this plate can be calculated by means of the above formulae.

9. Determination of Ratios of Elastic Constants from Observation of Dislocations in the Electron Microscope

As the stress field of dislocations in an anisotropic solid depends on the elastic constants of the material, one can determine the values of certain combinations of these constants from dislocation configurations observed in the electron microscope. These configurations are mainly extended dislocations at the boundary of a stacking fault.

The evaluation is carried out by introducing the observed geometrical data into the equations of equilibrium for the respective dislocation arrangements. In this way only the ratios of elastic constants are obtained, and not their absolute values. This is evident: an increase of all elastic constants and of the stacking fault energy by the same factor would not change the observed array of dislocations.

For hexagonal crystals, the system of elastic constants is given by the following matrix:

$$c_{ik} = \begin{matrix} c_{11} & c_{12} & c_{13} & 0 & 0 & 0 \\ & c_{11} & c_{13} & 0 & 0 & 0 \\ & & c_{33} & 0 & 0 & 0 \\ & & & c_{44} & 0 & 0 \\ & & & & c_{44} & 0 \\ & & & & & \frac{1}{2}(c_{11}-c_{12}) \end{matrix}.$$

As one can only hope to determine the ratios of the five independent constants, at least four independent experimental values are needed. On the other hand, in the expressions for the stress field of a screw dislocation ((17) and (18)) and for an edge dislocation (32), the following five combinations of the elastic constants appear:

$$C_1, \quad C_2, \quad \delta_1, \quad \delta_3, \quad \Delta .$$

As the stacking fault energy γ is not known in advance, the absolute values of C_2 and C_1 cannot be determined: one obtains only their ratio $C_2/C_1 = 1 - \nu$. So there are four experimental data available, just sufficient to determine the four ratios of the elastic constants.

The stress field of a dislocation can be probed if an extended dislocations is observed, meeting a surface slightly inclined with respect to the basal plane. From the periodicity in contrast along the dislocation line, the distance from the surface of each point along the dislocation can be inferred. The ratio $C_2/C_1 = 1 - \nu$ is most conveniently determined from curved ribbons far away from the surfaces of thick plates [8].

10. The "Refraction" of Dislocation Lines at Surface Steps. Snell's Law

Consider a dislocation line which is not too far away from a surface which contains a step. In the region at the one side of the step the dislocation is appreciably closer to the surface than in the region at the other side (see Fig. 6a). Because of the difference in elastic energy, a "refraction" of the dislocations is observed. A relation between the two angles θ_1 and θ_2 (see Fig. 6b) will be derived.

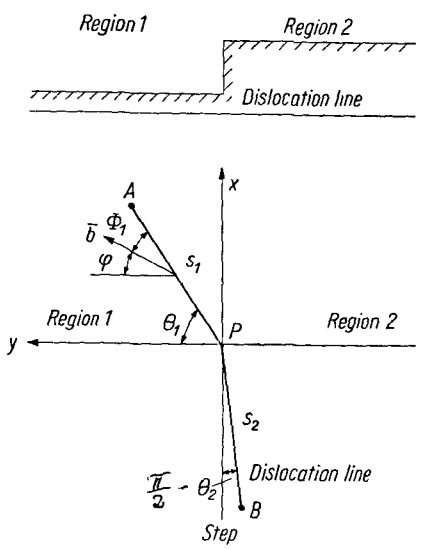

Fig. 6. "Refraction" of a dislocation passing beneath a surface step
a) cross section,
b) as seen from above.
The notation used in the text is indicated

The fine structure of the dislocation line in the immediate vicinity of the surface step (i. e., of the point P) will not be discussed, which means that the vertical dimensions (step height h and distance z of the dislocation from the nearest surface) are small as compared to any horizontal dimensions. In this case, we may assign two line energies ε_1 and ε_2 to the dislocation in the two regions. These line energies are, in general, functions of the orientation of the dislocation lines with respect to the Burgers vectors, i. e. $\varepsilon_1 = \varepsilon_1(y')$ and $\varepsilon_2 = \varepsilon_2(y')$.

The total energy of the dislocation between points A and B is then

$$E = \int_{x_A}^{x_P} \varepsilon_1(y') \sqrt{1 + y'^2}\, dx + \int_{x_P}^{x_B} \varepsilon_2(y') \sqrt{1 + y'^2}\, dx . \qquad (38)$$

This energy has to be minimized.

Let us assume that the position of the point P were already known. Then both integrals in equation (38) may be minimized separately. As the integrand is a function of y' only, y' is constant in each of the two regions. The dislocation consists, therefore, of two straight lines. In this case, the line energy is constant over the whole length of each of the two parts, and the total energy is given by

$$E = s_1\varepsilon_1 + s_2\varepsilon_2 = \sqrt{x_A^2 + y_A^2}\,\varepsilon_1 + \sqrt{x_B^2 + y_B^2}\,\varepsilon_2 . \quad |x_A| + |x_B| = L = \text{const} . \tag{39}$$

That value of x_B has to be determined which minimizes E in equation (39). The line energy ε on either side of the step is the sum of the line energies of the screw- and edge-parts

$$\varepsilon = \varepsilon_S \cos^2 \Phi + \varepsilon_E \sin^2 \Phi ,$$

where ε_S and ε_E are the energies of the dislocation in screw and edge position (see chapter 5). Introducing the angles θ and ψ, according to $\Phi = \theta - \varphi$, and substituting

$$\sin\theta = \frac{|x|}{\sqrt{x^2 + y^2}} \qquad \text{and} \qquad \cos\theta = \frac{|y|}{\sqrt{x^2 + y^2}} ,$$

one obtains

$$s\,\varepsilon = \frac{y^2\,a}{\sqrt{x^2 + y^2}} + \frac{x^2\,b}{\sqrt{x^2 + y^2}} + \frac{x\,y\,c}{\sqrt{x^2 + y^2}} ,$$

for each of the two lines, with

$$a = \varepsilon_S \cos^2\varphi + \varepsilon_E \sin^2\varphi ; \quad b = \varepsilon_S \sin^2\varphi + \varepsilon_E \cos^2\varphi ; \quad c = (\varepsilon_S - \varepsilon_E) \sin 2\varphi .$$

Substituting this into the minimum condition for E

$$\frac{\partial}{\partial x_A} E = 0 ,$$

we obtain, upon introducing again the angles θ_1 and θ_2

$$\begin{aligned} &\sin\theta_2 \left[-a_2 \cos^2\theta_2 + b_2 \sin^2\theta_2 + 2\,b_2 \cos^2\theta_2\right] + c_2 \cos^3\theta_2 \\ &\quad = \sin\theta_1 \left[-a_1 \cos^2\theta_1 + b_1 \sin^2\theta_1 + 2\,b_1 \cos^2\theta_1\right] + c_1 \cos^3\theta_1 . \end{aligned}$$

Introducing $u = \sin\theta$, one obtains

$$\frac{1}{2}\Sigma_2 u_2 + \Delta_2 f(u_2) = \frac{1}{2}\Sigma_1 u_1 + \Delta_1 f(u_1) \tag{40}$$

with

$$f(u) = \left(\frac{3}{2} - u^2\right) u \cos 2\varphi - (1 - u^2)^{3/2} \sin 2\varphi ; \quad \Delta = \varepsilon_E - \varepsilon_S ; \quad \Sigma = \varepsilon_E + \varepsilon_S .$$

For certain values of the elastic constants, the energies of edge and screw dislocations may be equal in both regions. In this case, $\Delta_1 = \Delta_2 = 0$, and equation (40) reduces to Snell's law of refraction

$$\varepsilon_1 \sin\theta_1 = \varepsilon_2 \sin\theta_2 .$$

The products of the sines of the "angles of incidence" times the line energies are equal. The "index of refraction" is the ratio of the self-energies in the two regions. The energies ε_1 and ε_2 usually differ not very much as a consequence of the logarithmic dependence on z. A visible effect will nevertheless result if the angle of incidence is not too small and if the change in distance to the nearest surface is appreciable.

11. Attachment of a Dislocation to a Surface Step

Dislocations crossing a surface step are sometimes observed to cling to the step for a certain distance (see Fig. 7). It is concluded from this observation that the energy of the dislocation in the immediate vicinity of the steps is decreased, probably due to the proximity of the extra surface at the step. In other words: there is a potential trough for the dislocation in the neighbourhood of the step.

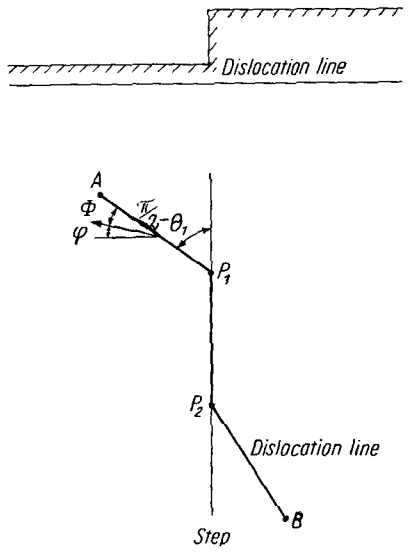

Fig. 7. "Capture" of a dislocation at a surface step
a) Cross section
b) as seen from above.
The notation used in the text is indicated

The width of this potential trough is assumed to be small as compared to horizontal dimensions. The energy of the dislocation at the bottom of the trough is denoted by ε_K. The same abbreviations as in chapter 8 are used.

The position of point P_1 which leads to a minimum of the total energy is given by

$$\frac{\partial E}{\partial x} = -\varepsilon_K + \frac{\partial}{\partial x}\varepsilon_1 s_1 = 0 .$$

This yields

$$\varepsilon_K = \frac{1}{2}\Sigma_1 u_1 + \Delta_1 f(u_1) .$$

Thus the angle θ is given as a function of material constants, of the angle φ, and of the distance z of the dislocation in region 1 from the surface. For a dislocation line anchored at two point A and B, the position of points P_1 and P_2 is uniquely determined. If the straight line connecting A and B encloses a large angle with the step the above derivation might yield the point P_2 to be to the left of point P_1. In this case the treatment of chapter 8 applies; the dislocation is then crossing the potential trough without being captured.

12. Observations

We shall now discuss a few observations which show unambigously that the corrections discussed above may become appreciable causing interesting effects. The observations were made on platelets of tin disulfide and tin sulfoselenide grown by sublimation.

12.1 Crystal structure

Tin disulfide and tin sulfoselenide belong to the hexagonal system: they have the cadmium iodide structure. The succession of layers in the c-direction can be described by means of the symbol

$$a\,\gamma\,b\,a\,\gamma\,b\,a\,\gamma\,b \ldots .$$

The latin letters represent sulfur or selenium, whilst the greek letters represent tin. The close-packed layers of tin atoms are sandwiched between two close-packed sulfur layers; they occupy the octahedral interstices. The binding between tin and sulfur (selenium) is probably stronger than between the two sulfur layers. Glide, therefore, takes place preferentially between two close-packed sulfur layers.

Consequently, the dislocations can dissociate into Shockley partials. The stacking fault between the two partials has the cadmium chloride structure. The stacking fault energy is small, and hence the ribbons are wide; in sufficiently thick crystals the width is about 0.25 μ.

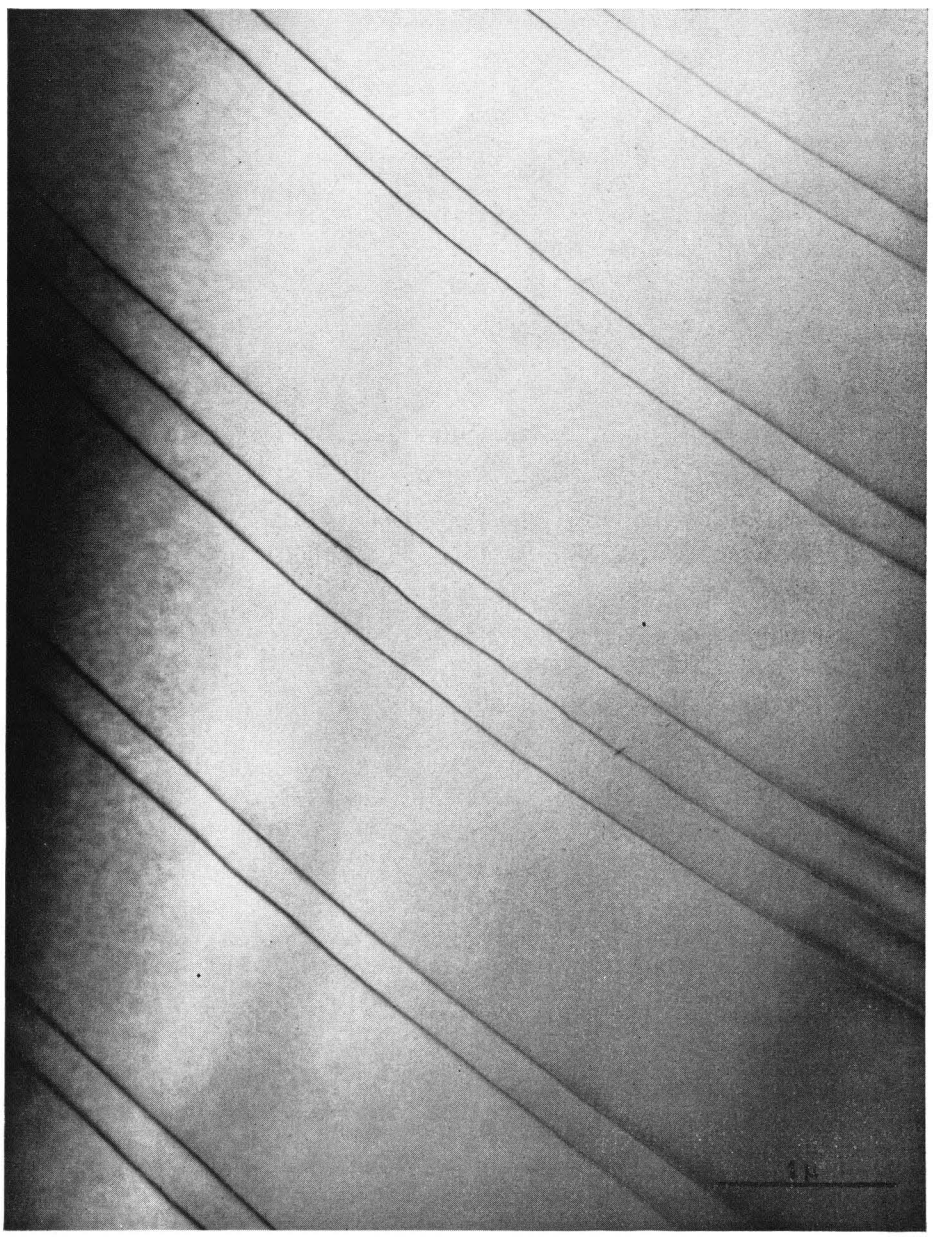

Fig. 8. Sequence of ribbons in tin disulfide single crystal. The width of the double ribbon is only three times wider than that of the single ones

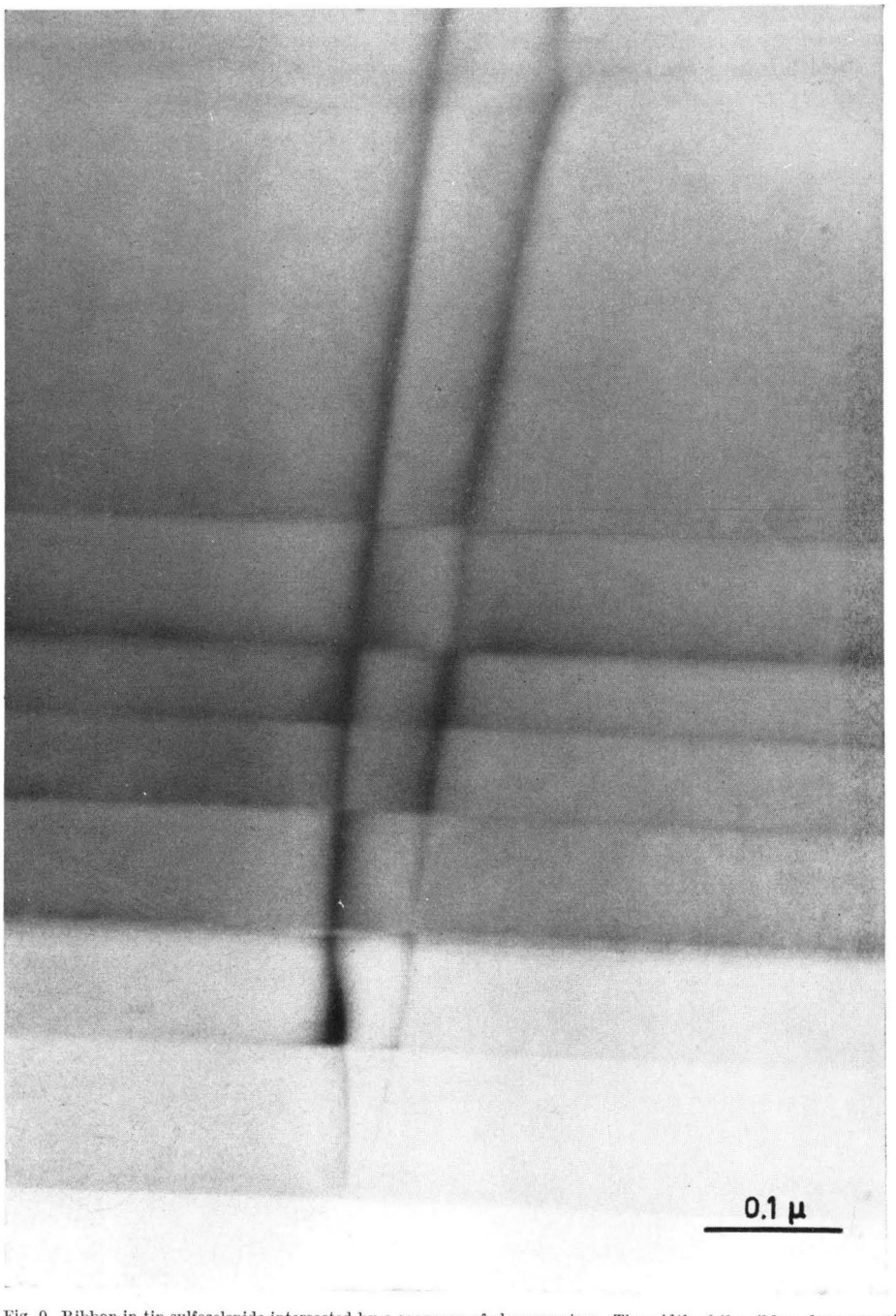

Fig. 9. Ribbon in tin sulfoselenide intersected by a sequence of cleavage steps. The width of the ribbon decreases at each step

12.2 Change in width of ribbons close to the surface

From the expressions (17) and (33) and from Fig. 4 and 5 it follows that the repulsion between partials becomes appreciably smaller than in an infinite crystal if the distance to the nearest surface is comparable to, or smaller than, the ribbon width. For very anisotropic substances like graphite, ($\Delta = 78$) the effect is small and the ribbon has to be very close to the surface in order to see any effect. For a material with intermediate anisotropy and which shows wide ribbons, i. e. has a small stacking fault energy, an appreciable variation of the ribbon width is to be expected, depending on the distance to the surface.

In tin disulfide and tin sulfoselenide, the widths of the ribbons are variable; even in the same specimen and for the same angle between Burgers vector and ribbon, the width may be different. In the same family of parallel ribbons the widths are usually equal, because the ribbons are also lying in the same glide plane (Fig. 8).

The double ribbons, consisting of three partials with the same Burgers vector, which are often observed in these substances, have a width which is only about three times that of single ribbons (Fig. 8). Isotropic theory predicts that, in an infinite solid, double ribbons should be about six times wider than single ones (equation (6) and (7)).

All these observations suggest that the ribbon widths are in the range where, for crystals of a thickness such that they can be examined in the electron microscope, surface effects become appreciable.

This could be checked directly by observing the changes in width with varying distance to the surface. Fig. 9 shows a ribbon in tin sulfoselenide intersected by cleavage steps. It is quite clear that the width decreases as the foil thickness, and hence the distance of the ribbon to the surface, diminishes.

Some of the crystals of sulfoselenide have smoothly sloping edges covered with growth steps, shown in cross section in

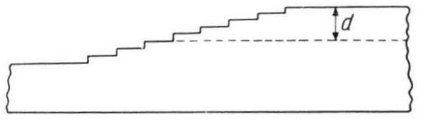

a)

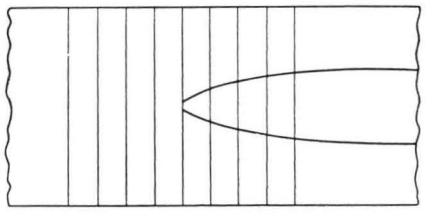

b)

Fig. 10a. Cross section of tapered crystal grown by sublimation

Fig. 10b. Top view of ribbon emerging in the tapered part

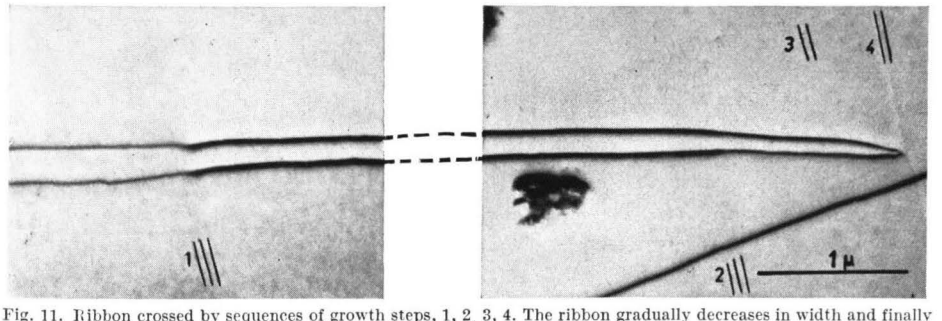

Fig. 11. Ribbon crossed by sequences of growth steps, 1, 2, 3, 4. The ribbon gradually decreases in width and finally the two partials coalesce

Fig. 10. Ribbons emerging in this tapered part become gradually narrower as they approach the surface. An example of this is seen in Fig. 11. Fig. 12 shows a double ribbon approaching gradually the surface, and finally emerging in it; its width decreases progressively. Fig. 13 finally shows single ribbons and one asymmetrical double ribbon crossed by growth steps along AB.

For a quantitative verification, the distance from the surface of each part of the ribbon has to be known. In principle, it is possible to measure this by making use of the alternating left-right contrast at dislocations which are oblique with respect to the surface [9, 10]. A striking example of this type of contrast is shown

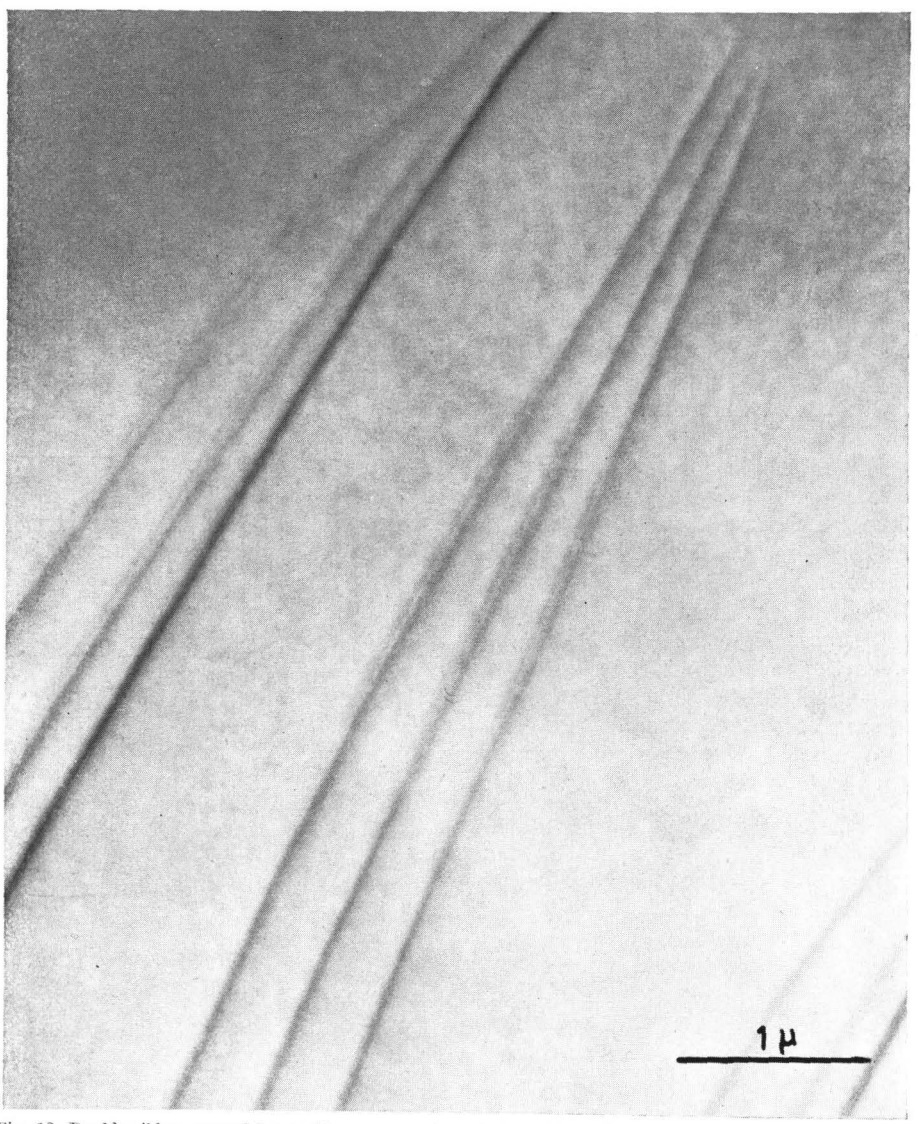

Fig. 12. Double ribbon crossed by a wide sequence of small steps. The width decreased very gradually, finally it emerges in the surface

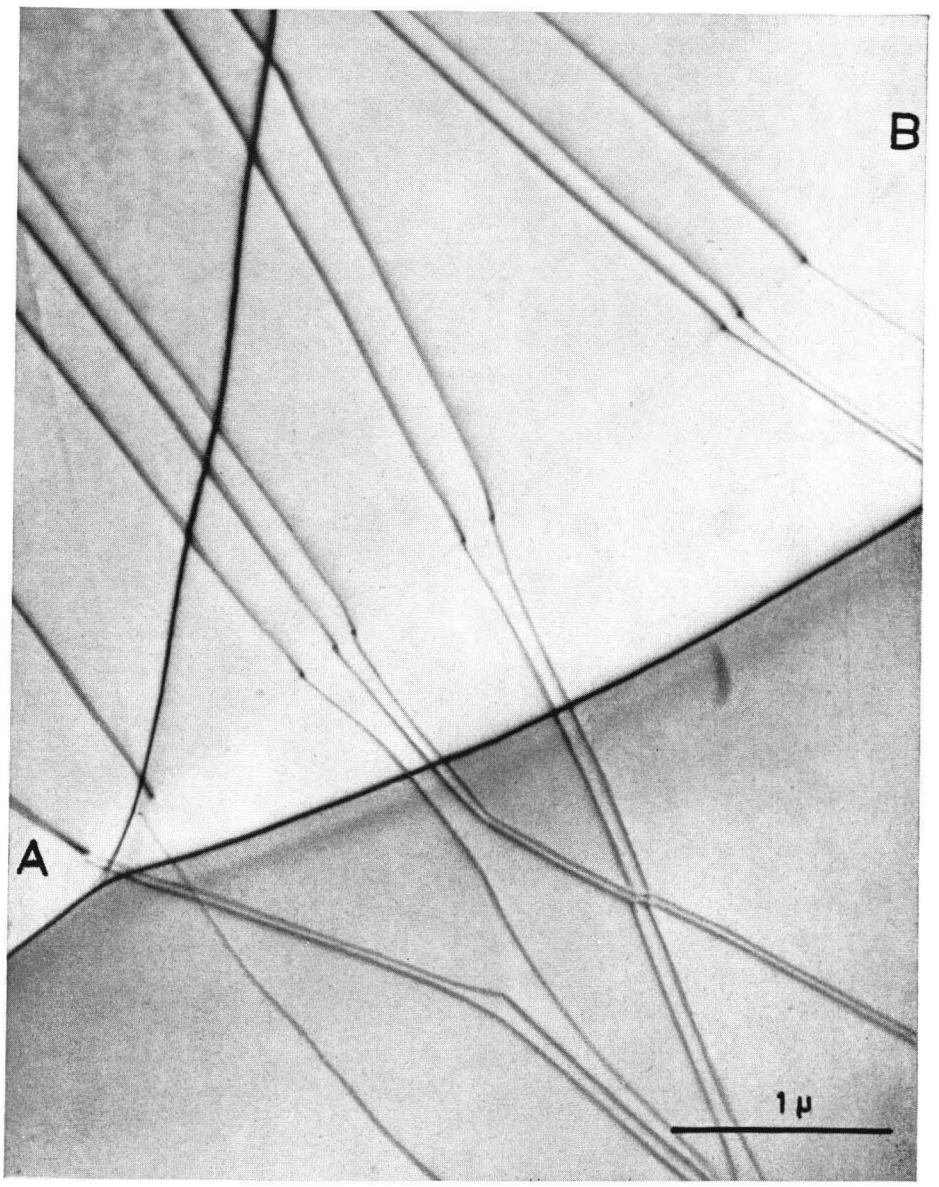

Fig. 13. Various ribbons crossed by a growth step along AB

in Fig. 14, together with the wedge fringes. The depth periodicity of this contrast is the same as that of the wedge fringes. For known contrast conditions, the depth of the dislocation below the surface can be calculated from this periodicity. Such measurements will be published in a separate paper.

12.3 The refraction effect

A particularly striking example of the refraction effect, observed in tin sulfoselenide, is reproduced in Fig. 15. A family of ribbons is crossed obliquely by two

steps one along AB, the other along CD. The change in direction at AB is accompanied by a change in width.

In region I the ribbons are widest, which means that their distance from the surface is larger there than in region II. This is in agreement with the observation

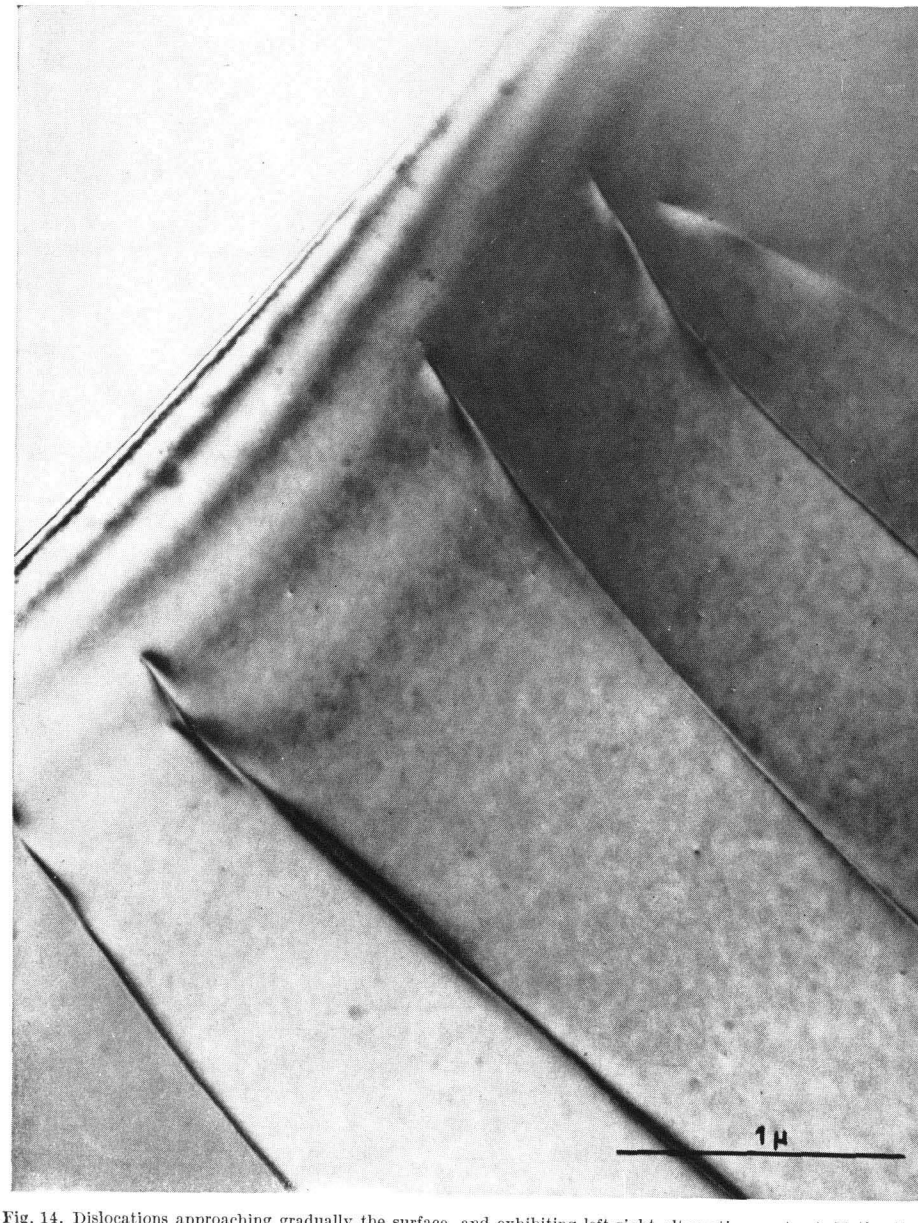

Fig. 14. Dislocations approaching gradually the surface, and exhibiting left right alternating contrast. Notice that in any given region the periodicity of the left-right contrast is the same as that of the wedge fringes. This phenomenon can be used to determine the depth of a dislocation below the surface

Fig. 15. "Refraction" of a family of ribbon and of unextended dislocations by two sequences of steps AB and CD. On refraction the ribbon width changes as well

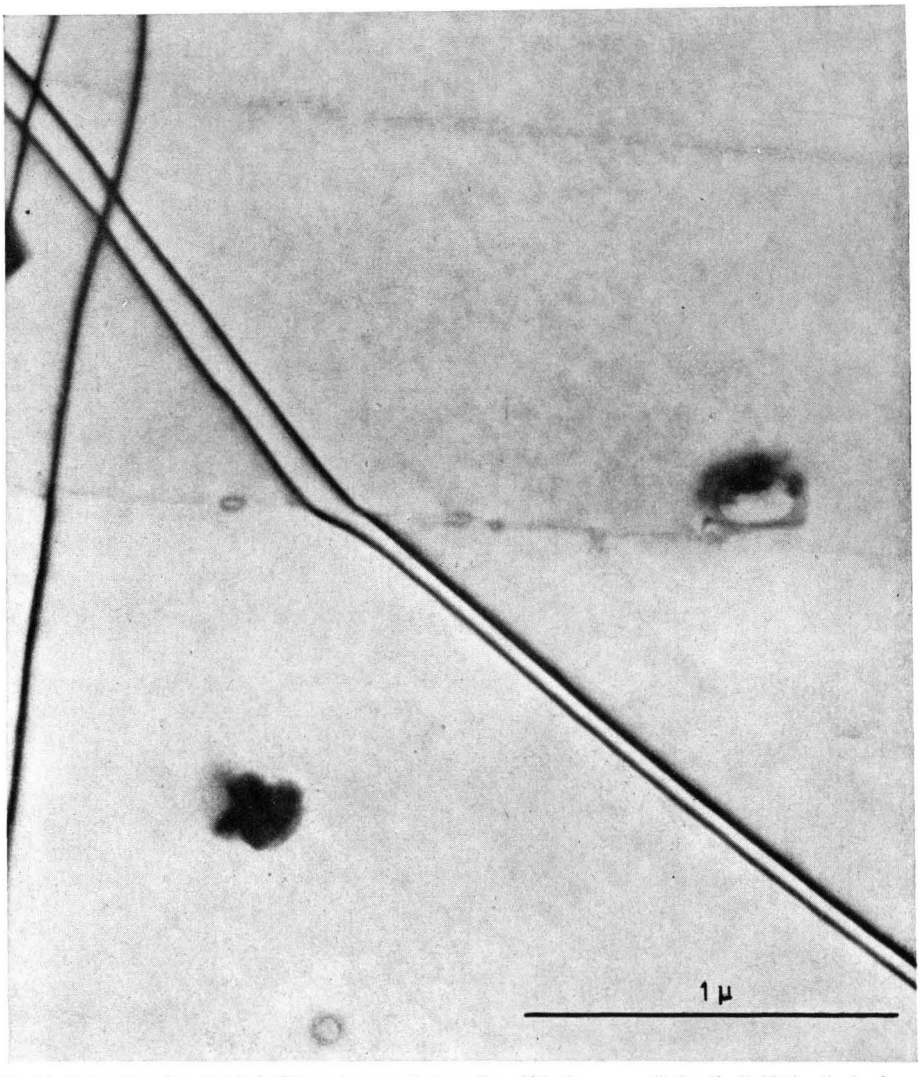

Fig. 16. Refraction of an isolated ribbon at a growth step; the width changes on "refraction". Notice the tendency of the partials to align with the step

that in region I the angle between the ribbons and the normal to the step is also larger than in region II.

Fig. 16 shows an isolated ribbon which is refracted by the step XY; notice the tendency to align with the steps.

12.4 Interaction of dislocations with surface steps

Fig. 17 shows finally an example of the effect discussed in chapter 11. A family of undissociated dislocations is deflected by a sequence of steps in the band AB. At first the dislocations are refracted, but finally the angle of incidence becomes too close to 90°, and the dislocations now cling to the steps over a considerable length.

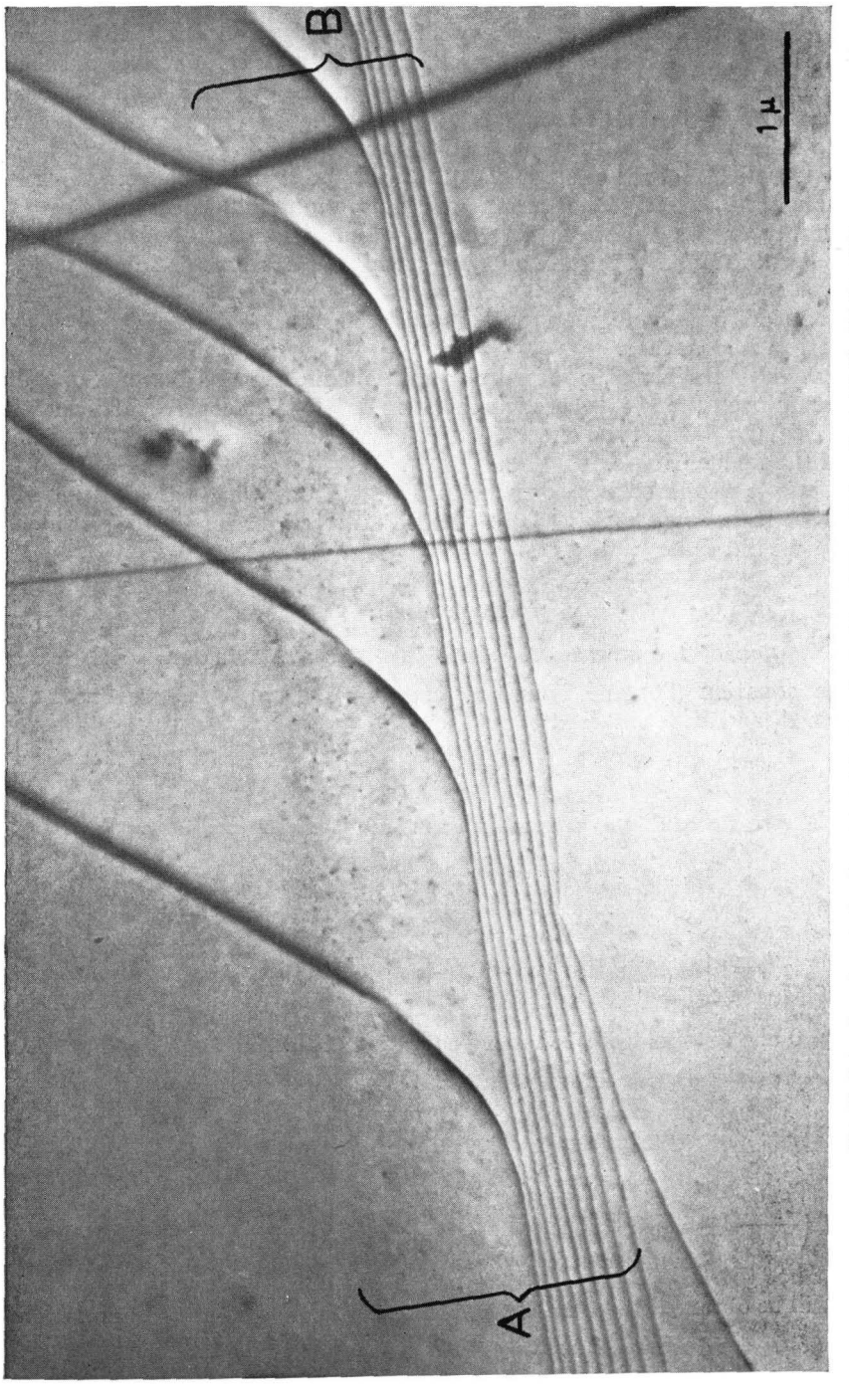

Fig. 17. Refraction of a set of undissociated dislocations by a wide sequence of steps along AB. Finally the angle of incidence becomes too large and the dislocations now follow the step direction

13. Conclusions

Expressions are derived for the stress fields of edge and screw dislocations in the basal plane of hexagonal semi-infinite crystals. The self-energies of such dislocations are calculated as well; they depend on the distance of the dislocation from the surface. The theory predicts a visible change in width for ribbons coming close to the surface. Observations confirm this.

The dependence of the energy of a dislocation on its distance from the surface is demonstrated directly by observing the "refraction" of dislocations where they cross growth or cleavage steps. To a first approximation this "refraction" follows Snell's law, the index of refraction being the ratio of the energies on both sides of the step.

Dislocations tend to align on growth steps; this effect is due to interaction with the vertical step surface.

A method is indicated to measure in particular cases the distance of a dislocation from the surface, it is based on the periodic left-right contrast at dislocations. The periodicity of this type of contrast is shown experimentally to be the same as that of the wedge fringes.

The effects described here demonstrate that if one wishes to use the ribbon widths for measuring stacking fault energies, corrections for finite foil thickness have in general to be applied.

Appendix I

Determination of the stress field which satisfies the boundary conditions (20)

From equation (26) and boundary conditions (20a), the following relation between A_1 and A_2 is obtained

$$A_1 = -A_2 \frac{R_2}{R_1} .$$

Thus the stresses can be expressed in terms of A_2 alone

$$\tau^C_{zx} = -i\sqrt{\delta_1}\, R_2 \int_{-\infty}^{\infty} \alpha\, |\alpha|\, A_2 \left(e^{-|\alpha|\sqrt{\delta_1} R_1 z} - e^{-|\alpha|\sqrt{\delta_1} R_2 z}\right) e^{i\alpha x}\, d\alpha , \tag{A1}$$

$$\tau^C_{zz} = \int_{-\infty}^{\infty} \alpha^2 A_2 \left(\frac{R_2}{R_1} e^{-|\alpha|\sqrt{\delta_1} R_1 z} - e^{-|\alpha|\sqrt{\delta_1} R_2 z}\right) e^{i\alpha x}\, d\alpha . \tag{A2}$$

For $z = 0$ one obtains from boundary condition (20b)

$$\tau^B_{zz} = \int_{-\infty}^{\infty} \alpha^2 A_2(\alpha) \left(\frac{R_2}{R_1} - 1\right) e^{i\alpha x}\, dx ,$$

i. e.

$$\alpha^2 A_2(\alpha) \left(\frac{R_2}{R_1} - 1\right) = \frac{1}{2\pi} \int_{-\infty}^{\infty} \tau^B_{zz}\, e^{-i\alpha x}\, dx = \frac{2 C_1 b_E \bar{\zeta}}{2\pi} \int_{-\infty}^{\infty} \frac{x^2 - \bar{\zeta}^2}{x^4 + A\, x^2 \bar{\zeta}^2 + \bar{\zeta}^4} e^{-i\alpha x}\, dx . \tag{A3}$$

$A_2(\alpha)$ will be obtained by complex integration. The integrand has simple poles at

$$x = i\bar{\zeta} R_1 , \quad x = -i\bar{\zeta} R_1 , \quad x = i\bar{\zeta} R_2 , \quad x = -i\bar{\zeta} R_2 ,$$

where R_1 and R_2 are given by equation (23).

For $\alpha < 0$ the path of integration is taken to be the real axis and in the upper half plane a half circle whose radius is going to infinity. The value I_1 of the integral in equation (A3) is[4])

$$I_1 = 2\pi i\,(\text{Res}\; i\bar{\zeta} R_1 + \text{Res}\; i\bar{\zeta} R_2) = \frac{\pi}{\bar{\zeta}\,(R_1^2 - R_2^2)}\left[\frac{R_1^2+1}{R_1}\, e^{\bar{\zeta} R_1 \alpha} - \frac{R_2^2+1}{R_2}\, e^{\bar{\zeta} R_2 \alpha}\right].$$

From the definition of R_1 and R_2 (equation (23)), one obtains

$$R_1^2\, R_2^2 = 1 \tag{A4}$$

and

$$\frac{R_1^2+1}{R_1} = \frac{R_2^2+1}{R_2} = R_1 + R_2\,. \tag{A5}$$

Thus

$$I_1 = \frac{\pi}{\bar{\zeta}}\,\frac{1}{R_1 - R_2}\left[e^{\bar{\zeta} R_1 \alpha} - e^{\bar{\zeta} R_2 \alpha}\right].$$

For $\alpha > 0$ the path of integration is taken in the lower half plane. Bearing in mind that the path of integration is now described clockwise, we obtain in this case

$$I_2 = \frac{\pi}{\bar{\zeta}}\,\frac{1}{R_1 - R_2}\left[e^{-\bar{\zeta} R_1 \alpha} - e^{-\bar{\zeta} R_2 \alpha}\right].$$

The following formula is valid for positive and negative values of α:

$$I = \frac{\pi}{\bar{\zeta}}\,\frac{1}{R_1 - R_2}\left[e^{-\bar{\zeta} R_1 |\alpha|} - e^{-\bar{\zeta} R_2 |\alpha|}\right].$$

The two functions $A_1(\alpha)$ and $A_2(\alpha)$ are

$$A_2(\alpha) = \frac{-C_1\, b_E\, R_1}{\alpha^2\,(R_2 - R_1)^2\sqrt{\delta_1}}\left[e^{-\bar{\zeta} R_1 |\alpha|} - e^{-\bar{\zeta} R_2 |\alpha|}\right]$$

and

$$A_1(\alpha) = -\,(R_2/R_1)\, A_1(\alpha)\,. \tag{A6}$$

Appendix II

The stress formula in the limit of isotropy

In the isotropic case, the elastic constants are given by the scheme

$$C_{ik} = \begin{pmatrix} \lambda+2\mu & \lambda & \lambda & 0 & 0 & 0 \\ & \lambda+2\mu & \lambda & 0 & 0 & 0 \\ & & \lambda+2\mu & 0 & 0 & 0 \\ & & & \mu & 0 & 0 \\ & & & & \mu & 0 \\ & & & & & \mu \end{pmatrix}.$$

In terms of λ and μ, Poisson's ratio can be expressed as $\nu = \lambda/2\,(\lambda+\mu)$. The values of the parameters defined in equation (10) are then

$$\delta_1 = 1\,, \qquad \delta_2 = 2\,, \qquad \delta_3 = 1\,,$$

$$\Delta = 2\,, \qquad C_1 = \frac{\mu}{2\pi}\,\frac{1}{1-\nu}\,, \qquad C_2 = \frac{\mu}{2\pi}\,.$$

[4]) The residue of the integrand at a point x is denoted by Res x.

Thus, for isotropy one has

$$z' = \bar{z} = z\,.$$

The equation for the stress due to a screw dislocation (equation (16)) then becomes

$$\tau_{xy} = \frac{\mu}{2\pi}\left[\frac{x}{x^2+(z-\zeta)^2} - \frac{x}{x^2+(z+\zeta)^2}\right], \tag{A7}$$

which is identical with the formula for the isotropic case given by DIETZE and LEIBFRIED [1].

The corresponding formula for the edge dislocation is obtained from equation (30) by taking the limit

$$\Delta - 2 \equiv \varepsilon^2 \to 0$$

Then one finds

$$R_1^2 \to 1 + \varepsilon + \frac{\varepsilon^2}{2}; \qquad R_2^2 \to 1 - \varepsilon - \frac{\varepsilon^2}{2};$$

$$R_1 \to 1 + \frac{\varepsilon}{2} + \frac{\varepsilon^2}{8}; \qquad R_2 \to 1 - \frac{\varepsilon}{2} + \frac{\varepsilon^2}{8}.$$

The terms $N_\pm$ in equation (30) are transformed into

$$N_\pm = [x^2 - (z \pm \zeta)^2] \cdot [x^2 + (z \pm \zeta)^2]^{-2};$$

and the terms I_{ij} into

$$I_{ij} = \frac{1}{A}\left\{1 - \frac{\varepsilon(\zeta+z)(\pm\zeta\pm z) + \frac{\varepsilon^2}{4}[(\pm\zeta\pm z)^2 + (\zeta+z)^2]}{A} + \frac{\varepsilon^2(\zeta+z)^2(\pm\zeta\pm z)^2}{A^2}\right\},$$

with

$$A = (\zeta+z)^2 + x^2\,.$$

For $i \neq j$ the variables ζ and z have opposite sign, for $i = j$ they have the same sign. Introducing these expressions into equation (30) yields

$$\tau_{zx} = \frac{\mu\, b_E\, x}{2\pi(1-\nu)}\left\{-\frac{(z-\zeta)^2 - x^2}{[(z-\zeta)^2+x^2]^2} + \frac{(z+\zeta)^2 - x^2}{[(z+\zeta)^2+x^2]^2} - 4\zeta z\frac{3(\zeta+z)^2 - x^2}{[(z+\zeta)^2+x^2]^3}\right\}$$

in full agreement with DIETZE and LEIBFRIED's formula.

References

[1] H. DIETZE and G. LEIBFRIED, Diplomarbeit, Göttingen 1949.
[2] J. D. ESHELBY, W. T. READ, and W. SHOCKLEY, Acta metall. **1**, 251 (1953).
[3] A. SEEGER and G. SCHÖK, Acta metall. **1**, 519 (1953).
[4] G. B. SPENCE, to be published.
[5] C. BAKER, Y. T. CHOU, and A. KELLY, Phil. Mag. **6**, 1305 (1961).
[6] G. B. SPENCE, 5th Biennal Conference on Carbon, Pennsylvania State University, June 19—23, 1961.
[7] R. SIEMS, Diskussionstagung über Strahlungsschäden und Plastische Verformung, Göttingen, Oktober 1961.
[8] R. SIEMS, P. DELAVIGNETTE, and S. AMELINCKX, Z. Phys. **165**, 502 (1961).
[9] P. B. HIRSCH, A. HOWIE, and M. J. WHELAN, Phil. Trans. Roy. Soc. **252**, 499 (1960).
[10] A. HOWIE, and M. J. WHELAN, Proc. of the European Regional Conference on Electron microscopy, Delft, **1**, 194 (1960).

(Received March 19, 1962)